ISSN 0010-9525, Cosmic Research, 2018, Vol. 56, No. 6, pp. 488–497. © Pleiades Publishing, Ltd., 2018.

Monitoring of Natural and Technogenic Space Hazards: Results of the *Lomonosov* Mission and *Universat-SOCRAT* Project

V. A. Sadovnichii[a], M. I. Panasyuk[a], V. M. Lipunov[a], A. V. Bogomolov[a], V. V. Bogomolov[a], G. K. Garipov[a], E. S. Gorbovskoy[a], D. S. Zimnukhov[a], A. F. Iyudin[a], M. A. Kaznacheeva[a], V. V. Kalegaev[a], P. A. Klimov[a], A. S. Kovtukh[a], V. G. Kornilov[a], N. V. Kuznetsov[a], I. A. Maksimov[a], S. K. Mit[a], V. I. Osedlo[a], V. L. Petrov[a], M. V. Podzolko[a], E. P. Popova[a], A. Yu. Poroykov[a], I. A. Rubinstein[a], K. Yu. Saleev[a], S. I. Svertilov[a, *], V. I. Tulupov[a], B. A. Khrenov[a], V. V. Chazov[a], A. S. Chepurnov[a], Ya. A. Shtunder[a], A. N. Shustova[a], and I. V. Yashin[a]

[a] *Moscow State University, Moscow, 119991 Russia*

**e-mail: sis@coronas.ru*

Received December 3, 2017

Abstract—The results of experiments onboard the *Lomonosov* satellite on observing natural and technogenic space hazards including electromagnetic transients and space debris are discussed. A new space project *Universat-SOCRAT* being developed by Moscow State University is also discussed. The project aims to create a constellation of small satellites for real-time monitoring of the radiation environment and potentially hazardous objects of natural (asteroids, meteoroids) and technogenic origin (space debris) in near-Earth space, and such phenomena as cosmic and atmospheric gamma-ray bursts and optical and ultraviolet radiation flashes from Earth's atmosphere.

DOI: 10.1134/S001095251901009X

INTRODUCTION

The natural and technogenic space environment poses significant risks for space missions, both robotic and manned. The risks depend on parameters of planned missions: duration, location in outer space, and orbital parameters.

Specific natural conditions in outer space (diverse physical parameters of radiation fields as well as features of ballistic trajectories of natural space objects) and consequences of human activity in space (space pollution with technogenic debris) pose, as a rule, a real challenge for modeling the situation and calculating risks. Real-time monitoring of natural and technogenic space objects, i.e., potential hazards, represents an optimal and effective way to reduce risks.

Experiments onboard the Russian *Lomonosov* satellite involve, along with astrophysical tasks [1], investigation and monitoring of radiation environment, atmospheric electromagnetic transient phenomena (hereinafter, transients or TAP), and space debris in near-Earth space, which bear potential hazards for space missions. This article presents some of the results of these experiments.

Results of experiments onboard the *Lomonosov* satellite and other satellites launched by Moscow State University (MSU) to study extreme phenomena in Earth's atmosphere and outer space [2–5] shaped the framework of a new MSU project named *Universat-SOCRAT*[1], which aims to create a constellation of satellites for close-to-real-time monitoring of potential hazards in near-Earth space, including: radiation environment, hazardous objects of natural (asteroids, meteors) and technogenic origin (debris), and electromagnetic transients, i.e., space and atmospheric gamma-ray bursts and optical and UV flashes from Earth's atmosphere. The goals and objectives of this project, as well as the basic requirements for new instruments, are also discussed in this article.

If successful, the project will create the world's first prototype of a space system for monitoring and preventing space hazards both for ongoing and planned space missions, including high-altitude atmospheric aircraft.

1. POTENTIAL HAZARDS IN NEAR-EARTH SPACE

1.1. Ionizing Radiation

One of the main damage effects for performance of space instruments and for safety of manned missions is charged high-energy particle (protons and elec-

[1] Abbreviation "Universat"—University Satellite; "SOCRAT"—System of Observing the Cosmic Radiation, Asteroid and Technogenic hazard.

trons) fluxes from Earth's radiation belts as well as energetic particles of solar cosmic rays. These fluxes experience very significant variations on a time scale from milliseconds to tens of years, which cannot be described by existing quasi-static models of Earth's radiation belts (see, e.g., [6–8]). On the other hand, satellite measurements are now conducted only for a limited number of orbits and a limited range of pitch angles (the angle between the particle velocity vector and magnetic force line) and cannot provide a global picture of space–time radiation variations in near-Earth space (NES). Therefore, a need arises for radiation monitoring and operational forecasting of Earth's radiation environment for the following purposes:

—Operational assessment of the radiation environment in NES to assess the radiation risks of space missions and develop alert signals for mission control decision making.

—Verification of modern computational models of radiation fields in NES.

1.2. Space Debris, Asteroids, and Large Meteoroids

As of August 31, 2015, a total of 17250 space objects of technogenic origin were located in outer space and cataloged in the Warning Systems for Hazards in Near-Earth Space databases. Of these, 1362 space objects were operational spacecraft, and the remaining 15888 space objects were space debris [9].

Extrapolations of existing rates of pollution in low near-Earth orbits, even if various measures are taken to reduce it, show a possible cascade effect in the medium term due to mutual collisions of objects and space-debris particles. In the long run, this effect may lead to a catastrophic increase in the population of objects in low orbits and, consequently, make further space exploration virtually impossible.

Also relevant is the issue of asteroid hazard. A celestial body is considered potentially hazardous if it crosses Earth's orbit at a distance less than 0.05 AU (~19.5 Earth–Moon distances) and its diameter exceeds 100–150 m. Objects of this size are large enough to cause unprecedented destruction on land, or a huge tsunami if they fall into the ocean. Events of this magnitude occur about once every 10000 years. Based on the information obtained from the *Wide-Field Infrared Survey Explorer* (*WISE)* space telescope, experts estimate a population of 4700 ± 1500 potentially hazardous objects with diameters of more than 100 m [10].

1.3. Electromagnetic Transients

Another potentially hazardous phenomenon is electromagnetic transients in the upper atmosphere, which are observed in different wavelength ranges: from the radio to gamma range. Of these, fairly reliably identified in experiments are transient luminous events (TLEs), i.e., light flashes predominantly in the near UV and red ranges, and terrestrial gamma flashes, i.e., gamma-ray bursts of terrestrial origin. These phenomena may be associated with high-altitude electrical discharges arising from an impact on the mesosphere by avalanches of runaway electrons or caused by energetic electrons precipitated from radiation belts and electromagnetic waves occurring at altitudes of tens of kilometers in the upper atmosphere and are global in nature [11–17]. The energy release in these phenomena is large enough to have a significant impact on radio communications, modify physical parameters of the mesosphere, and have a direct impact on onboard systems of stratospheric suborbital aircraft (see, e.g., [18]).

Cosmic gamma-ray bursts of astrophysical origin may also pose a potential hazard (see, e.g., [19]). Despite having very remote sources, gamma-ray bursts are, in fact, the most powerful processes in the Universe, like a hypernova explosion, merging of neutron stars, or a collapse of a magnetar's magnetic field. The effect of these rare yet very intense cosmic gamma-ray bursts on Earth's atmosphere is so far little understood, but it can be comparable with solar flares in terms of ionospheric disturbances.

1.4. Anthropogenic Sources of Ionizing Radiation in NES

Radionuclide energy sources and nuclear propulsion systems of spacecraft pose a potential hazard for other spacecraft located near the former. Detection and determination of physical characteristics of nuclear-active spacecraft is an important element of radiation risk mitigation [20, 21].

2. OBSERVATIONS OF POTENTIALLY HAZARDOUS PHENOMENA IN EXPERIMENTS ONBOARD THE *LOMONOSOV* SATELLITE

2.1. Lomonosov Mission

The *Lomonosov* satellite was launched on April 28, 2016 from the Vostochny Cosmodrome into a circular solar-synchronous orbit with an altitude of ~500 km, an inclination of 98°, and an orbital period of ~90 min. The scientific payloads onboard *Lomonosov* include the Trekovaya Ustanovka (TUS) space telescope to record tracks of extensive air showers (EASs) from cosmic rays of extremely high energies by ionization luminescence [22] and a set of instruments for studying cosmic gamma-bursts, including BDRG X-ray and gamma-ray detectors [23], SHOK wide-field optical cameras [24], and UFFO ultraviolet and X-ray telescope [25]. All the instruments operate in a continuous measurement mode and, therefore, can simultaneously record events, including in the optical, UV, X-ray, and gamma ranges.

2.2. Observations of Transient Atmospheric Phenomena

Observations of atmospheric electromagnetic transients in the optical and UV ranges were completed using the TUS orbiting telescope. TUS is the world's first instrument designed to record tracks of extremely high energy cosmic rays (EHECRs), i.e., particles with energies greater than 7×10^{19} eV, in Earth's atmosphere onboard an artificial satellite. However, the measurement technique enables investigation of various fast processes in the atmosphere on different time scales (see below).

TUS is a mirror telescope consisting of a large-area (~2 m^2) Fresnel-type concentrating mirror and a photodetector located in the focal plane. The photodetector is a matrix of $16 \times 16 = 256$ photomultiplier tubes (PMTs) of the Hamamatsu R1463 type. Each PMT is furnished with a filter that transmits only UV radiation in the range 240–400 nm. The solid viewing angle of the cell is 10^{-4} sr, which corresponds in the atmosphere to observation of a 5×5 km square [22, 26].

The TUS detector can operate in four modes with different time resolutions and time-base lengths (see Table 1). Therefore, the TUS detector can be used to investigate various phenomena in Earth's atmosphere. The first mode serves for recording EASs from EHECRs and short (less than 1 ms) transients; the second and third modes, for measuring lightning discharges and TAP; the fourth mode, for recording meteors and thunderstorms lasting longer than 1 s.

Several classes of flashes with a characteristic temporal structure [27] were identified in events recorded with the TUS detector. Thunderstorms are the main source of short-term UV radiation in the atmosphere, which is recorded with the detector in all modes. Thus, the TUS detector enables observation of lightning discharges with different time resolutions. Figure 1 shows characteristic signals during the recording of lightning discharges for three operation modes of the detector: (a) events recorded in the EAS mode (with a time resolution of 0.8 μs), which show a smooth increase in the signal for 100 μs; (b) events with a pronounced time structure, which were recorded in the Long TAP mode (with a time resolution of 0.4 ms); (c) multipeak structure of thunderstorm activity in the Micrometeors mode (with a time resolution of 6.6 s).

Analysis of the spatial structure of the events showed that most of them are recorded by the entire photodetector simultaneously and have no apparent signal center, i.e., show some kind of uniform light exposure. The most natural explanation for this effect is that the detector reacts to flashes outside the field of view and the uniform signal throughout the photodetector is due to the scattering of UV radiation from rough mirror surfaces. Indeed, preflight tests showed that the proportion of focused light in the image is 60%. This means that the remaining 40% of the UV signal hitting the mirror is evenly scattered and illuminates all photodetector cells.

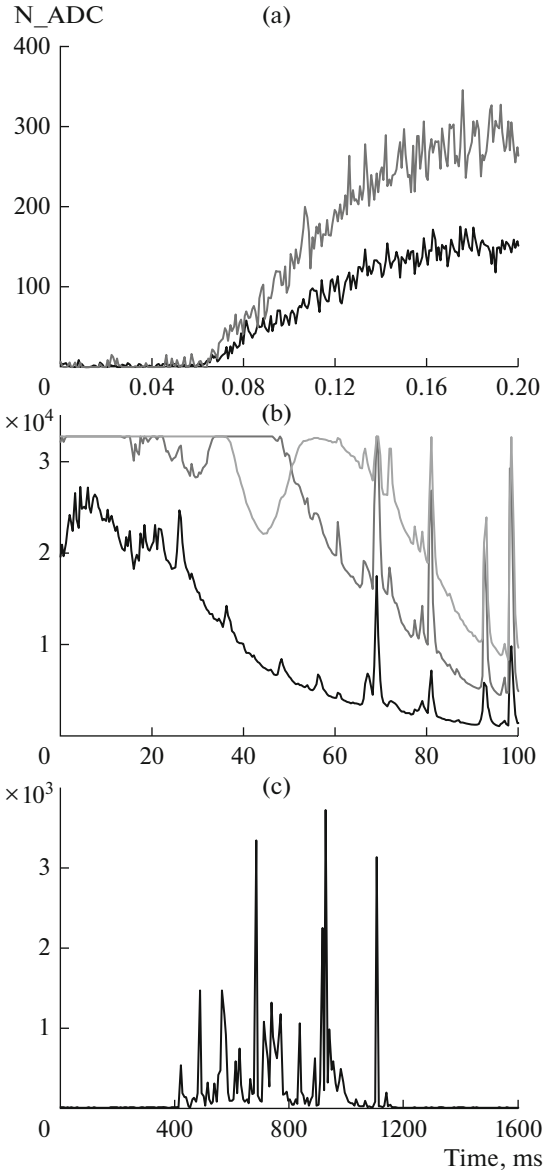

Fig. 1.

Since the TUS telescope has a spatial resolution, some types of TAP were reliably identified from characteristic spatial–temporal patterns. Specifically, this concerns elves-type events. More than 15 high-atmospheric transient elves events were recorded during the operation of the TUS detector onboard the *Lomonosov*

Table 1. Time parameters of different operation modes of the TUS detector

Operation mode	Time resolution, τ	Time base
EAS	0.8 μs	256 τ = 205 μs
Short TAP	25.6 μs	256 τ = 6.6 ms
Long TAP	0.4 μs	256 τ = 105 ms
Micrometeors	6.6 ms	256 τ = 1.7 s

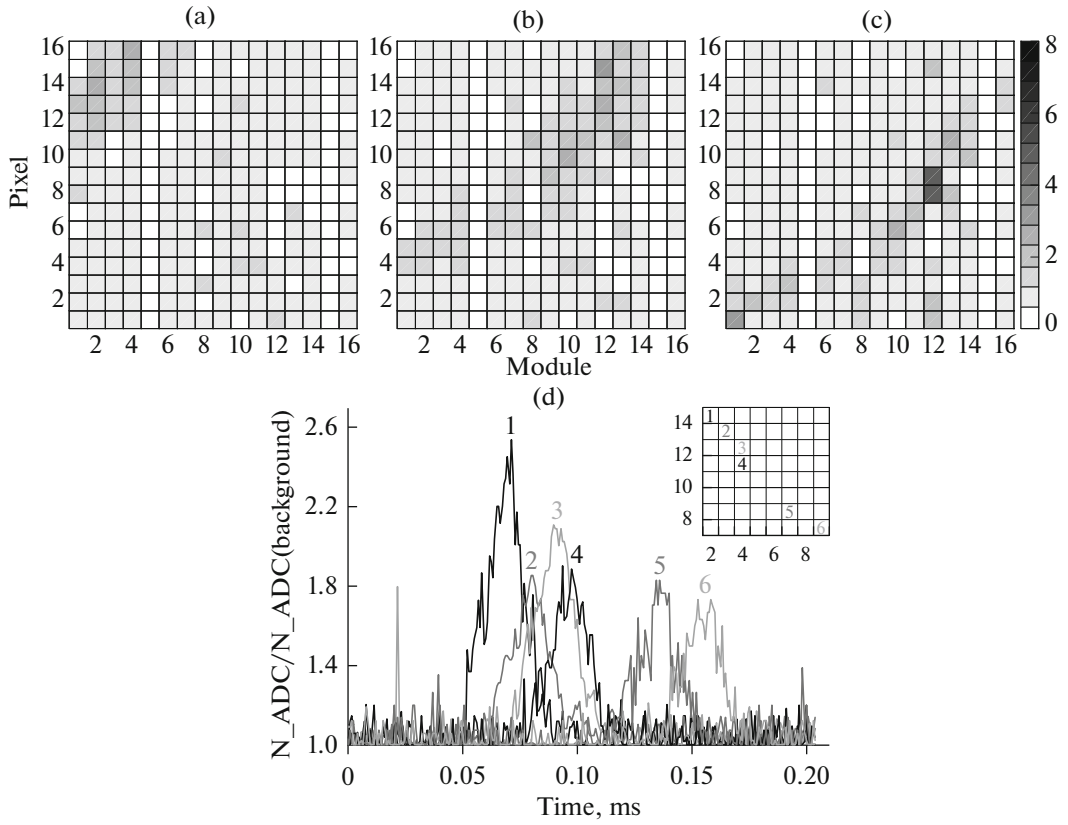

Fig. 2. Sample recording of an elves-type TAP with the TUS detector: (a)–(c) maps of the photodetector matrix channels at 0.077, 0.174, and 0.182 ms from the start of event recording; (d) time profiles for several specified pixels of the photodetector. The geographical coordinates of the event: 17° E, 9° N.

satellite. A sample recording is shown in Fig. 2. These events have the shape of an expanding ring 100–400 km in diameter. Flashes of this kind are well identified in the experimental data set from the characteristic shape of the signals in the detector channels, which line up in an arc running across the photodetector matrix (Figs. 2a–2c). Elves last less than a millisecond; therefore, their dynamics are clearly visible in the detector mode with a time resolution of 0.8 μs (EAS mode) and indiscernible in other modes.

2.3. Observations of Meteors and Space Debris

TUS can be used in principle for meteor observations and has, to this end, a special mode (see Table 1). Efficiency of ground-based meteor observations is limited mainly by changes in weather conditions while orbital experiments have no such disadvantage. The meteor mode of TUS provides a time resolution of 6.6 ms with a complete recording of a digitized signal (oscillogram) lasting 1.7 s. This mode is slower than those used to observe EASs and electromagnetic transients. It can also record the long-term glow structure of a thunderstorm region and glow of technogenic origin. More or less typical meteors with velocities on the order of 3×10^6 cm/s can be efficiently recorded using TUS from the fluorescent glow arising along the meteor track with a threshold kinetic energy of 25 J at a digitization period of about 10 ms [28].

Dozens of meteors were detected within a month of operation in the meteor mode. Observation results for one of the events are presented in Fig. 3. The velocity of the meteor under the assumption of horizontal motion within the field of view of the TUS telescope was 50–60 km/s. The meteor was recorded on January 3, 2017 at 14:31:08 UTC, at the maximum intensity of the Quadrantide meteor shower in 2017.

These measurements demonstrate the possibilities of using an orbital fluorescent EHECR detector for studying meteors, which confirms the strategy and estimates for the next-generation orbital JEM-EUSO detector, designed for studying meteors [19, 30]. This telescope was shown to observe meteors with brightness up to a magnitude of $M = +7$. Given the large field of view and high recording efficiency, the JEM-EUSO telescope will ensure recording of a substantial stream of meteors, both single events and meteor showers.

The *Lomonosov* satellite was also used for onboard optical observations of space objects of artificial origin, including space debris. The observations employed the SHOK-1 and SHOK-2 optical cameras with a wide

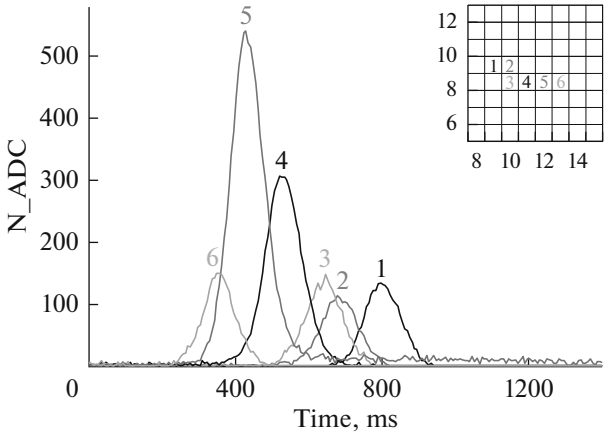

Fig. 3. Waveforms of the light-exposed pixels in the photodetector unit of the TUS instrument during the recording of the meteor event on January 3, 2017, 14:31:08 UTC.

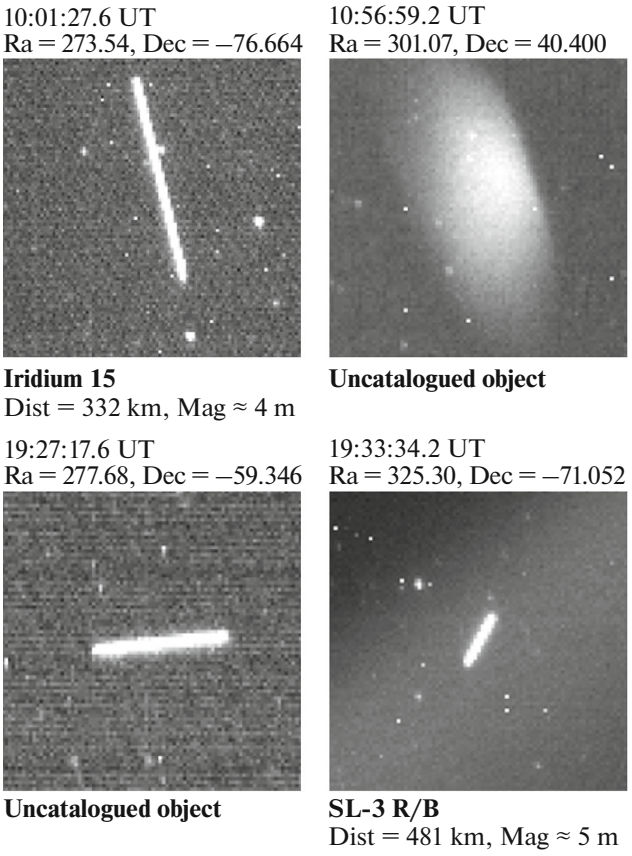

Fig. 4.

field of view. Both units are connected directly to the central onboard electronics unit, which runs communications with the onboard systems and other instruments in the complex. These are cameras of the same type as those used in the ground-based MASTER robotic telescope network to search for optical transients, including short gamma-ray bursts [31, 32].

Each camera is based on a Nikkor lens and Kodak KAI-11002 CCD. The cameras have a sensitivity of magnitude $9–10^m$. Each camera is oriented in such a way that its field of view stays within the field of view of one of the BDRG gamma-ray detectors. The units continuously record images with a time resolution of 0.2 s. If a trigger arrives from the BDRG units or UBAT X-ray telescope of the UFFO instrument, data are recorded 1 min before and 2 min after the trigger. Due to coaxiality with BDRG gamma-ray detectors, this scheme enables recording short gamma-ray bursts simultaneously with both instruments and capturing an optical image both at the time of the burst and prior to it. Selected time intervals for data recording overlap the typical times between the precursor and the burst. It is also possible to capture SHOK images by a trigger from the Earth, i.e., by bursts detected by the global GCN network. Cameras can also make observations in the optical transient search mode, i.e., by their own trigger. In this case, each subsequent image is automatically compared with the previous one also if brightness changes or a new object appears, and the field of view of the camera is fixed. This mode can be used not only for observations of astrophysical phenomena such as supernovae and novae but also for the study of space debris, meteorite hazards, etc.

Examples of identification of fast-moving objects on May 14, 2016 using the wide-field optical cameras onboard the *Lomonosov* satellite are shown in Fig. 4.

3. CONCEPT OF A SPACE EXPERIMENT BASED ON A SMALL SATELLITE CONSTELLATION FOR SPACE HAZARD MONITORING

3.1. Small Satellite Constellation for Space Hazard Monitoring

Based on the experience accumulated during observations onboard the *Lomonosov* satellite, a new project named *Universat-SOCRAT* is proposed to monitor potentially hazardous phenomena using several small satellites [33]. The minimal option suggests using a constellation of three satellites: Satellite 1 is put in a low Sun-synchronous orbit with an altitude of 500–650 km and inclination of 97°–98°; Satellite 2 is launched into near-circular orbit with an altitude of 1400–1500 km and inclination of ~80°; and Satellite 3, into an elliptical orbit with an apogee of 8000 km, perigee of 600–700 km, and inclination of 63.4°. The relative positions of the orbits are shown in Fig. 5.

The following instruments for monitoring hazardous objects and phenomena are to be installed onboard the satellites: spectrometer of protons and electrons (SPE) [34], wide-field optical cameras, and a set of instruments for studying electromagnetic transient phenomena, including gamma spectrometers and UV and IR detectors. Satellite 1 should carry the following payloads: instruments for monitoring space

radiation, a set of instruments for optically monitoring hazardous objects, a set of science payloads for studying TAP in the optical range, a set of science payloads for monitoring the gamma range, and a data collection unit (DCU). Both Satellites 2 and 3 should carry instruments for monitoring cosmic radiation; possibly, a wide-field optical camera and a compact gamma-spectrometer; and an electronics unit to communicate with onboard satellite systems. The science payloads should also include a DCU to acquire scientific and telemetric information from individual instruments and transfer it to an onboard storage device as well as send power and commands to the instruments from the onboard satellite systems.

3.2. Instruments for Monitoring Radiation

The equipment for monitoring cosmic radiation should include a spectrometer of protons in the energy range from 1 to >160 MeV and electrons in the energy range of 0.15–10 MeV. Its main element is a telescope-type assembly, which includes several semiconductor detectors of various thicknesses and a scintillation detector, which are installed coaxially one under another (Fig. 6, left panel). Several telescopes with different spatial orientation are used to measure the pitch-angle flux distribution and omnidirectional particle fluxes. One earlier scheme of the instrument is shown in Fig. 6 (right panel). Later another scheme has been considered, where the axes of four telescopes lie in the plane of the magnetic meridian (in the case of a near-polar orbit of the satellite, this means that they must lie almost in the orbital plane) and the axis of another telescope is perpendicular to the plane of the magnetic meridian.

The above orbital parameters for the satellites with instruments for radiation monitoring cover the wide spatial range of existence of radiation trapped in a magnetic field, i.e., radiation belts. The satellites should measure the omnidirectional fluxes of trapped particles with subsequent interpolation and extrapolation of the fluxes to the wide region of the radiation belts using the known theoretical and empirical dependencies. These measurements allow to calculate of the current distribution of particle fluxes in a large volume of radiation belts and, consequently, the current levels of radiation loads for a large range of operating orbits.

The payloads should also include a three-component magnetometer.

An important addition to the space monitoring system is developed in Moscow University fully automated ground-based system for operational analysis of satellite data, which is designed to assess and predict radiation environment in NES in real time.

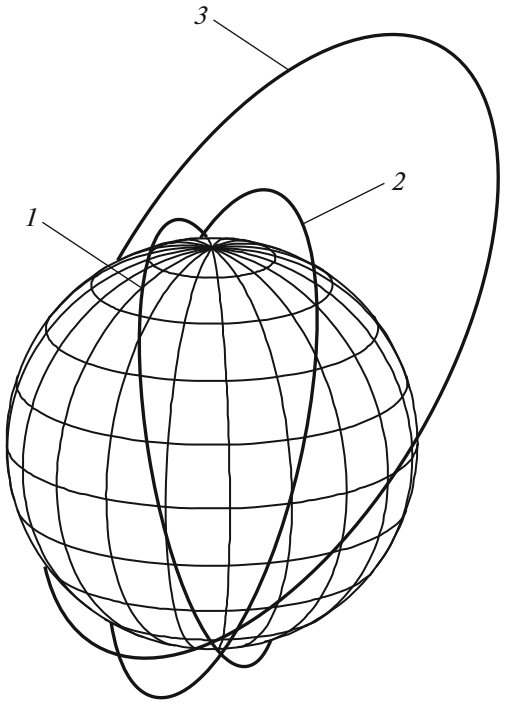

Fig. 5.

3.3. Instruments for Optically Monitoring Hazardous Objects

The set of instruments for optical monitoring of hazardous objects should consist of two wide-field optical cameras (mini-telescopes) and a scanning telescope with an input window diameter of 120–250 mm and a working field of view up to 100 square degrees. As noted above, cameras of this type are successfully used onboard the *Lomonosov* satellite. Data from each camera should be analyzed using a processor that performs both detailed recording of a video sequence (5 fps) by a trigger from a gamma-ray detector or another instrument (gamma-ray bursts) and sampling of video fragments related to spacecraft, space debris, asteroids, and other objects. For observations to be successful, one should have means of stabilizing telescope orientation for the time of exposure (up to 3 min) with an accuracy of no worse than 5″ relative to fixed stars and possess knowledge of the telescope orientation at the starting time of exposure no worse than 60′.

The *Universat-SOCRAT* satellite constellation should conduct monitoring in a close-to-real-time mode. To this end, it is planned to involve other spacecraft (e.g., *Globalstar* or *Gonets* satellites or telecommunication satellites in geostationary orbit). It is also planned to conduct joint monitoring of potentially hazardous objects in space using the *Universat-SOCRAT* space segment and ground-based MASTER robotic telescope network, which has been deployed in different countries [31, 32].

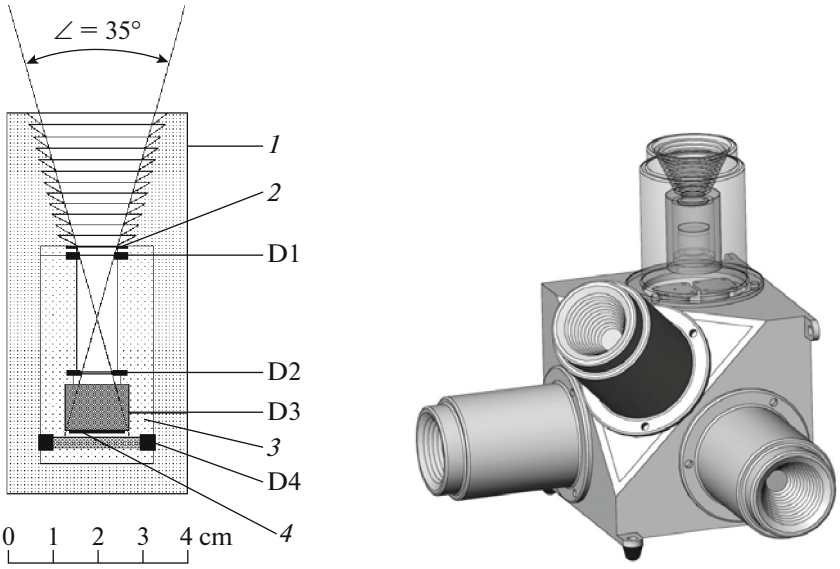

Fig. 6. Left: design scheme of the SPE telescope: (*1*) housing; (*2*) foil ≈10 μm; (*3*) insulator; D1, D2, and D4 are semiconductor (Si) detectors; D3 is a scintillation (CsI(Tl)) detector; (*4*) photodiode. Right: variant of the SPE detector unit with differently directed telescopes.

3.4. Instruments for Monitoring Electromagnetic Transients

The set of science payloads for studying TAP in both UV and optical ranges should include a spatially sensitive spectrometer, i.e., a small lens telescope (SLT) with high time resolution for measuring the optical radiation spectra of TAP and lightning strikes, and DUFIK UV and IR detectors, i.e., an analogue of the detectors onboard the *Tatyana* and *Vernov* satellites [35, 36] (for comparing the data from the new satellite with the previous ones), supplemented by measurement channels in the far UV range. Spectral measurements are necessary to determine the type and altitude of TAP generation and identification of lightning discharges by the characteristic line, 777 nm, and by the absence of a signal in the region of the oxygen absorption line, 762 nm. The axes of the SLT and DUFIK instruments should be oriented to the nadir with nonshading angles of 90° along the detector axes. The SLT should consist of a wide-field lens, a position-sensitive detector in the form of a multianode photomultiplier, and a set of photomultipliers for measuring long time series of the TAP signal with high sensitivity and high time resolution. The design of the instrument includes up to 16 spectral channels.

The DUFIK instrument should consist of three photomultipliers, whose input windows are shielded with light filters to ensure operation in different spectral ranges: infrared (600–800 nm), near UV (240–400 nm), and Sun-blind (100–300 nm). In addition, its composition should include an optical detector based on a microchannel plate to ensure detection of radiation from far UV to soft X-rays.

The set of science payloads for monitoring the gamma range should include three BDRG-type omnidirectional scintillation gamma-ray detectors [37] for monitoring the upper atmosphere and for sky surveys in the range 10–3000 keV and a high-resolution and high-sensitivity tracking gamma spectrometer. The detector node of each BDRG unit represents an assembly of a thin (0.3 cm) NaI (Tl) scintillator and a thicker (1.7 cm) CsI (Tl) scintillator of cylindrical shape. Both scintillation crystals have the same diameter of 13 cm and are viewed by one photomultiplier, i.e., the so-called phoswich. The axes of the three BDRG-type gamma detectors should be perpendicular to one another and directed along the mutually perpendicular edges of the cube, as if forming a Cartesian coordinate system. The main diagonal of the cube should be oriented to the nadir.

The high-resolution and high-sensitivity tracking gamma spectrometer is a combination of a position-sensitive detector with a coding mask. The instrument also includes a hodoscopic node based on scintillation fibers. The instrument axis should be oriented along the nadir–zenith axis: the instrument should be oriented to the zenith on the side of the coding mask and to the nadir on the side of the hodoscope node. The effective area of the gamma spectrometer is ~250 cm^2; the energy range is 50–5000 keV (in the coding mode, 50–1000 keV); the angular resolution is ~2°; and the field of view of full coding is ±25°. The gamma telescope can verify the appearance of a point source and, thus, separate gamma-ray bursts of various nature from particle dropouts. The payloads also include a data analysis unit containing digital electronics nodes allowing one to record readings with high time resolu-

tion (up to 10 μs), conduct operational analysis of images from the telescope with a coding mask, and generate a gamma-ray trigger.

3.5. Ground Control

During the space experiment, it is planned to set up a ground control unit for controlling the satellites as well as receiving and processing relevant scientific data. The unit will be part of the *Lomonosov* ground science complex, designed to ensure proper usage of the science payloads: receiving, processing, archiving, and disseminating information from the spacecraft. The ground control unit will establish the groundwork for implementation of the new MSU project *Universat-SOCRAT*, largely reducing project costs. This way we could avoid costs associated with the development of main spacecraft supports, i.e., command–program, information–telemetry, and navigation–ballistic systems.

Along with the system for receiving and processing space telemetry, MSU has designed a system for operational analysis and forecasting of radiation conditions in NES, based on automated analysis of space monitoring data using operational models of external space environment factors [38]. Their use will increase the efficiency of the *Universat-SOCRAT* space system.

CONCLUSIONS

It follows from the above that electromagnetic transients represent a potentially hazardous factor in near-Earth space and in Earth's upper atmosphere. The flash energy can be estimated, e.g., from the data on the UV radiation of TAP, which were obtained onboard MSU satellites, assuming that the number of UV photons is proportional to the ionization energy: $Q_a = E_{ion}/K(H)\varepsilon$, where Q_a is the number of UV photons; E_{ion} is the ionization energy; $K(H)$ is a proportionality coefficient; and ε is the energy of a single photon, 3.5 eV. The proportionality coefficient depends on altitude and is 10^3 for altitudes on the order of 50 km [39].

Based on the experimental distribution of TAP by the number of photons [40], this value lies in the range of 10^{23}–10^{25} photons, which yields an average energy per event on the order of 100 MJ. The lower-bound estimate for TAP energy release, which was obtained in the ISUAL experiment, is 700 MJ/min. If we compare the energy density (W/m^2) released in the atmosphere due to TAP with other light processes such as auroras, it will be two orders of magnitude higher (albeit on a small-time scale), which shows the importance of these processes for the upper atmosphere. Moreover, the frequency and intensity of high-altitude atmospheric transients can be a response to an external impact, i.e., an indicator of space weather.

Electromagnetic transients may also be sources of radiation hazard. During the development of TAP, electrons are accelerated to high energies (runaway electrons). These electrons have relativistic energies as high as several MeV, and dose effects of this radiation pose potential hazard for electronic systems. Estimates for effective radiation doses and for effects of runaway electron doses on human tissues for aircraft altitudes were obtained in [41]. It was shown that single-event doses obtained in these estimates are not hazardous for humans. However, dose estimates may change if one considers the spatial structure of the discharge. This factor is especially critical in the early stages of development of an electrical discharge, when its area is highly localized. One should also bear in mind that TAP often form in series (several events follow in succession within a short period of time), which may also cause an increase in the dose effect.

Another source of radiation hazard for spacecraft and aircraft may come from neutrons generated as a secondary component of TAP (see [42, 43]). Neutrons are generated in photonuclear interactions when the photon energy is above the photonuclear reaction threshold (about several MeV). Photons (gamma quanta) of such high energy are detected in the atmosphere, and these phenomena are called terrestrial gamma-ray flashes. The quantity of terrestrial gamma-ray flashes with a total energy of gamma quanta greater than 1 kJ is estimated in the literature at 10^{-5} km^{-2} per hour, with the expected quantity of neutrons per event being about 10^{12} (or the neutron flux from an object with dimension of 10 × 10 km being $\approx 10^4$ neutron/m^2). This neutron flux is an order of magnitude larger than that generated in an ordinary atmosphere due to the passage of cosmic rays; moreover, low-energy neutrons, which provide the main radiation effect, are not considered. In [43], an estimate was obtained for the dose from terrestrial gamma-ray flashes: the dose is 10^{-4} Sv near the source and drops to 10^{-10} at an altitude of 50 km. Importantly, radiation shields are less effective in the case of a neutron flux than in the case of charged particle (electron) fluxes.

Based on the results of observations of potentially hazardous cosmic phenomena onboard the *Lomonosov* satellite, including studies of electromagnetic transients, a new project was proposed, *Universat-SOCRAT*, which is aimed at addressing the following tasks:

—Operational (real-time) evaluation of radiation conditions in NES to assess radiation risks of space missions and generate alert signals for mission control decision making.

—Verification of modern computational models of radiation fields in NES.

—Real-time monitoring of potentially hazardous objects of natural and technogenic origin in NES.

—Monitoring of electromagnetic transients in Earth' upper atmosphere and in outer space (gamma-ray bursts, solar flashes).

Successful implementation of the project will achieve the following outcomes:

—The world's first prototype of a space system for monitoring and preventing space hazards for both ongoing and planned space missions, including high-altitude atmospheric aircraft.

—New innovative instrumentation technologies and new methods for solving information problems in real time.

—New educational standards and methods for training specialists in the new field of applied space research.

ACKNOWLEDGMENTS

This work was supported by Russia's Ministry of Education and Science (unique project ID: RFMEFI60717X0175).

REFERENCES

1. Sadovnichy, V.A., Panasyuk, M.I., Amelushkin, A.M., et al., Lomonosov satellite—space observatory to study extreme phenomena in space, *Space Sci. Rev.*, 2017, vol. 212, nos. 3–4, pp. 1705–1738.
2. Sadovnichii, V.A., Amelyushkin, A.M., Angelopoulos, V., et al., Space experiments aboard the Lomonosov MSU satellite, *Cosmic Res.*, 2013, vol. 51, no. 6, pp. 427–433.
3. Panasyuk, M.I., Svertilov, S.I., Bogomolov, V.V., et al., Experiment on the *Vernov* satellite: Transient energetic processes in the Earth's atmosphere and magnetosphere. Part I: Description of the experiment 2016, *Cosmic Res.*, 2016, vol. 54, no. 4, pp. 261–269.
4. Panasyuk, M.I., Svertilov, S.I., Bogomolov, V.V., et al., Experiment on the *Vernov* satellite: Transient energetic processes in the Earth's atmosphere and magnetosphere. Part II: Final results, *Cosmic Res.*, 2016, vol. 54, no. 5, pp. 343–350.
5. Sadovnichii, V.A., Panasyuk, M.I., Yashin, I.V., et al., Investigations of the space environment aboard the *Universitetsky–Tat'yana* and *Universitetsky–Tat'yana-2* microsatellites, *Sol. Syst. Res.*, 2011, vol. 45, no. 1, pp. 3–29.
6. Mullen, E.G., Gussenhoven, M.S., Ray, K., and Violet, M.A., A double-peaked inner radiation belt: Cause and effect as seen on CRRES, *IEEE Trans. Nucl. Sci.*, 1991, vol. 38, pp. 1713–1718.
7. Myagkova, I.N., Bogomolov, A.V., and Shugai, Yu.S., The dynamics of relativistic electron fluxes in the near-Earth space in 2001–2005, *Moscow Univ. Phys. Bull.*, 2010, vol. 65, no. 3, pp. 234–237.
8. Tverskaya, L.V., Balashov, S.V., Veden'kin, N.N., et al., Outer radiation belt of relativistic electrons during the minimum of the 23rd solar cycle, *Geomagn. Aeron. (Engl. Transl.)*, 2012, vol. 52, no. 6, pp. 740–745.
9. Harris, A., The population of near-Earth asteroids, *Icarus*, 2015, vol. 257, pp. 302–312.
10. Mainzer, A., Bauer, J., Grav, T., and Masiero, J., The population of tiny near-Earth objects observed by NEOWISE, *Astrophys. J.*, 2014, vol. 784, no. 2, id 110.
11. Gurevich, A.V., Milikh, G.M., and Roussel-Dupre, R.A., Runaway electron mechanism of air breakdown and preconditioning during a thunderstorm, *Phys. Lett. A*, 1992, vol. 165, nos. 5–6, pp. 463–468.
12. Mareev, E.A., Evtushenko, A.A., and Yashunin, S.A., On the modelling of sprites and sprite-producing clouds in the global electric circuit, in *Sprites, Elves and Intense Lightning Discharges*, Füllekrug, M., et al., Eds., Springer, Netherlands, 2006, pp. 313–340.
13. Milikh, G.M., Valdivia, J.A., and Papadopoulos, K., Spectrum of red sprites, *J. Atmos. Terr. Phys.*, 1998, vol. 60, nos. 7–9, pp. 907–915.
14. Surkov, V.V. and Hayakawa, M., Underlying mechanisms of transient luminous events: A review, *Ann. Geophys.*, 2012, vol. 30, no. 8, pp. 1185–1212.
15. Fishman, G.J., Bhat, P.N., Mallozzi, R., et al., Discovery of intense gamma-ray flashes of atmospheric origin, *Science*, 1994, vol. 264, no. 5163, pp. 1313–1316.
16. Dwyer, J.R., Smith, D.M., and Cummer, S.A., High-energy atmospheric physics: Terrestrial gamma-ray flashes and related phenomena, *Space Sci. Rev.*, 2012, vol. 173, nos. 1–4, pp. 133–196.
17. Dwyer, J.R., The relativistic feedback discharge model of terrestrial gamma ray flashes, *J. Geophys. Res.*, 2012, vol. 117, no. A2, A02308.
18. Garipov, G., Grigoriev, A., Khrenov, B., Klimov, P., and Panasyuk, M., High energy transient luminous atmospheric phenomena: The potential danger for suborbital flights, in *Extreme Events in Geospace*, Buzulukova, N., Ed., Elsevier, 2017, pp. 473–490.
19. Bhat, P.N., Meegan, C.A., von Kienlin, A., et al., The 3rd Fermi GBM gamma-ray burst catalog: The first six years, *Astrophys. J. Suppl. Ser.*, 2016, vol. 223, no. 2, id 28.
20. Radioactive space debris: what goes up, must come down, *WISE/NIRS Nuclear Monitor*, no. 629, June 10, 2005.
21. Anikeeva, M.A., Boyarchuk, K.A., and Ulin, S.E., Space debris detection onboard a space vehicle, *Vopr. Elektromekh.*, 2012, vol. 126, no. 1, pp. 13–18.
22. Klimov, P.A., Panasyuk, M.I., Khrenov, B.A., et al., The TUS detector of extreme energy cosmic rays on board the *Lomonosov* satellite, *Space Sci. Rev.*, 2017, vol. 212, nos. 3–4, pp. 1687–1703.
23. Svertilov, S.I., Panasyuk, M.I., Bogomolov, V.V., et al., Wide-field gamma-spectrometer BDRG: GRB monitor on-board the Lomonosov mission, *Space Sci. Rev.*, 2018, vol. 214, no. 1, id 8.
24. Lipunov, V.M., Gorbovskoy, E.S., Kornilov, V.G., et al., SHOK—the first Russian wide-field optical camera in space, *Space Sci. Rev.*, 2018, vol. 214, no. 1, id 6.
25. Park, I.H., Panasyuk, M.I., Reglero, V., et al., UFFO/*Lomonosov*: The payload for the observation of early photons from gamma ray bursts, *Space Sci. Rev.*, 2018, vol. 214, no. 1, id 14.
26. Adams, J.H. and the JEM-EUSO collaboration, Space experiment TUS onboard the Lomonosov satellite as pathfinder of JEM-EUSO, *Exp. Astron.*, 2015, vol. 40, no. 1, pp. 315–326.

27. Khrenov, B.A., Klimov, P.A, Panasyuk, M.I., et al., First results from the TUS orbital detector in the extensive air shower mode, *J. Cosmol. Astropart. Phys.*, 2017, vol. 2017, no. 9, id 006.

28. Khrenov, B.A. and Stulov, V.P., Detection of meteors and sub-relativistic dust grains by the fluorescence detectors of ultra high energy cosmic rays, *Adv. Space Res.*, 2006, vol. 37, no. 10, pp. 1868–1875.

29. Adams, J.H., Ahmad, S., Albert, J.N., et al., JEM-EUSO: Meteor and nuclearite observations, *Exp. Astron.*, 2015, vol. 40, no. 1, pp. 253–279.

30. Abdellaoui, G., Abe, S., Acheli, A., et al., Meteor studies in the framework of the JEM-EUSO program, *Planet. Space Sci.*, 2017, vol. 143, pp. 245–255.

31. Lipunov, V., Kornilov, V., Gorbovkoy, E., et al., Master robotic net, *Adv. Astron.*, 2010, id 349171.

32. Kornilov, V., Lipunov, V., Gorbovskoy, E., et al., Robotic optical telescopes global network master II. Equipment, structure, algorithms, *Exp. Astron.*, 2012, vol. 33, no. 1, pp. 173–196.

33. Panasyuk, M.I., Podzolko, M.V., Kovtyukh, A.S., et al., Operational radiation monitoring in near-Earth space based on the system of multiple small satellites, *Cosmic Res.*, 2015, vol. 53, no. 6, pp. 423–429.

34. Panasyuk, M.I., Podzolko, M.V., Kovtyukh, A.S., et al., Optimization of measurements of the Earth's radiation belt particle fluxes, *Cosmic Res.*, 2017, vol. 55, no. 2, pp. 79–87.

35. Garipov, G.K., Panasyuk, M.I., Rubinshtein, I.A., et al., Ultraviolet radiation detector of the MSU research educational microsatellite *Universitetskii–Tat'yana*, *Instrum. Exp. Tech*., 2006, vol. 49, no. 1, pp. 126–131.

36. Panasyuk, M.I., Svertilov, S.I., Bogomolov, V.V., et al., RELEC mission: Relativistic electron precipitation and TLE study on-board small spacecraft, *Adv. Space Res.*, 2016, vol. 57, no. 3, pp. 835–849.

37. Amelyushkin, A.M., Galkin, V.I., Goncharov, B.V., et al., The BDRG and SHOK instruments for studying gamma-ray burst prompt emission onboard the *Lomonosov* spacecraft, *Cosmic Res.*, 2013, vol. 51, no. 6, pp. 434–438.

38. Kalegaev, V.V., Bobrovnikov, S.Yu., Kuznetsov, N.V., Myagkova, I.N., and Shugai, Yu.S., The SIMP MSU operational space monitoring center, in *Prikladnye aspekty geliogeofiziki. Materialy spetsial'noi sektsii "Prakticheskie aspekty nauki kosmicheskoi pogody" 11-i ezhegodnoi konferentsii "Fizika plazmy v solnechnoi sisteme"* (Applied Aspects of Heliogeophysics: Proceedings of the Special Section "Practical Aspects of Space Weather" of the 11th Annual Conference "Plasma Physics in the Solar System"), Moscow: IKI RAN, 2016, pp. 146–159.

39. Belyaev, V.A. and Chudakov, A.E., Ionization glow of air and its possible use for air shower detection, *Izv. Akad. Nauk SSSR: Ser. Fiz.*, 1966, vol. 30, no. 10, pp. 1700–1707.

40. Klimov, P.A., Garipov, G.K., Khrenov, B.A., et al., Vernov satellite data of transient atmospheric events, *J. Appl. Meteorol. Climatol.*, 2017, vol. 56, no. 8, pp. 2189–2201.

41. Dwyer, J.R., Smith, D.M., Uman, M.A., et al., Estimation of the fluence of high-energy electron bursts produced by thunderclouds and the resulting radiation doses received in aircraft, *J. Geophys. Res.*, 2010, vol. 115, no. D9, D09206.

42. Tavani, M., Marisaldi, M., Labanti, C., et al., Terrestrial gamma-ray flashes as powerful particle accelerators, *Phys. Rev. Lett.*, 2011, vol. 106, no. 1, 018501.

43. Drozdov, A., Grigoriev, A., and Malyshkin, Y., Assessment of thunderstorm neutron radiation environment at altitudes of aviation flights, *J. Geophys. Res.*, 2013, vol. 118, no. 2, pp. 947–955.

Translated by A. Kobkova